Available online at www.sciencedirect.com
ScienceDirect
Solid State Communications 140 (2006) 144–148
solid state communications
www.elsevier.com/locate/ssc

Photonic band gaps in a two-dimensional photonic crystal with open veins

Wen-Long Liu*, Tzong-Jer Yang

Department of Electrophysics, National Chiao Tung University, Hsinchu 30050, Taiwan, ROC

Received 20 April 2006; received in revised form 2 August 2006; accepted 8 August 2006 by T. Ando
Available online 24 August 2006

Abstract

We report two-dimensional (2D) photonic crystals of a square lattice with square dielectric rods growing slender veins on the middle side of each square dielectric rod in air. The complete photonic band gap (PBG) is found in higher index bands. Then extending the length of veins substantially shrinks this PBG, and for an appropriate vein length creates the new complete PBG at lower index bands. But the greatest complete PBG can be gotten where the veins are not fully closed at the lattice unit cell boundary. The photonic band gap is the result of considering the effects of Mie scattering due to the slender veins and interference of electromagnetic waves. Our results may provide a new direction for designing PBG of 2D photonic crystals.

PACS: 42.70.Qs; 42.25.Bs; 41.20.-q

Keywords: A. Photonic crystals; A. Mie scattering; D. Photonic band gap

1. Introduction

Interest in the optical characteristics of materials has grown recently. So-called photonic crystals (PCs) exhibit photonic band gaps (PBGs) which inhibit the propagation of electromagnetic (EM) waves in any propagating direction and polarization state [1,2], leading to various peculiar physical phenomena [3] and providing potential applications [4–7]. The search for photonic crystals generating large PBGs is very important. Therefore, various two- and three-dimensionsal methods have been proposed and implemented [8,9]. For instance, Anderson and Giapis proposed to reduce the structural symmetry by introducing additional scatterers into the unit cell of the prototype lattices and thus lift the degeneracy of the photonic bands at the high symmetry points in the Brillouin zone [10]. Wang et al. suggested that to enhance the complete PBG by rotating noncircular air rods embedded in a dielectric background [11]. Another proposed approach is to break the degeneracy of photonic bands by employing dielectric anisotropy in the scattering elements, creating a large complete PBG in two-dimensional (2D) square and triangular lattices [12]. Other design schemes applying various materials and mechanisms have also been developed [13–19]. The interfacial layers etched between air rods and the background dielectric would not widen the complete band gap [20]; however, linking the dielectric rod with veins as a completely closed structure would give a large complete band gap [21], but it does not tell when the maximum complete PBG will occur. Recently, 2D photonic crystals consisting of a hexagonal array of circular rods connected with slender veins has been studied [22]. In addition, the search for three-dimensional (3D) PBG structures based on the six connected node simple-cubic-lattice dielectric networks has been proposed [23].

This work explores the square lattice with square rods growing slender veins on the middle side of each square dielectric rod in air. The veins were extended in length step by step until they touched and connected together. Band structures of the PCs were calculated using the plane-wave expansion method [24–26]. There exists one complete photonic band gap (PBG) in a higher frequency band of the prototype square lattices with only square rods [27]. When extending the slender veins, this PBG disappears gradually. The veins were found to be favor the creation of low-frequency complete band gaps. Numerical simulations show that another complete PBG opens while the length of veins continues to increase; then, it arrives

* Corresponding author. Tel.: +886 3 5720635; fax: +886 3 5725230.
E-mail address: wlliuz@ms48.hinet.net (W.-L. Liu).

0038-1098/$ - see front matter © 2006 Elsevier Ltd. All rights reserved.
doi:10.1016/j.ssc.2006.08.011

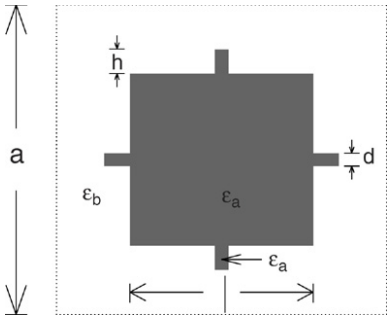

Fig. 1. Schematic diagram of the proposed photonic crystals. The square dielectric rod with a side-length l and dielectric ϵ_a is placed in air with $\epsilon_b = 1.0$ at the center of a 2D square lattice with a lattice constant, a, in the xy-plane. Another dielectric vein with $\epsilon = \epsilon_a$ and length h and width d is inserted in each unit cell on the middle of each side of the dielectric square rod, forming composite lattices.

at a maximum value where the veins are not completely closed at the lattice unit cell boundary. The photonic band gap is the result of considering the effects of Mie scattering [28] due to the slender veins and interference of EM waves. Our results may provide a new direction for designing PBG of two-dimensional photonic crystals.

2. Theory

Fig. 1 displays the schematic diagram of the proposed PC structure. The square dielectric rod with a side-length of l and dielectric ϵ_a is placed in an air background with $\epsilon_b = 1.0$ at the center of a 2D square lattice with a lattice constant, a, in the xy-plane. Another dielectric vein with $\epsilon = \epsilon_a$, length h and width d are placed in each unit cell on the middle of each side of the dielectric square rod, forming composite lattices.

The electromagnetic (EM) fields with E/H-polarization (in-pane magnetic/electric fields) in the 2D PC are governed by Maxwell's equations

$$\left\{\nabla \times \frac{1}{\epsilon(\mathbf{r})}\nabla\times\right\}\mathbf{H}(\mathbf{r}) = \frac{\omega^2}{c^2}\mathbf{H}(\mathbf{r}), \tag{1}$$

where $\mathbf{H}(\mathbf{r})$ denotes the magnetic fields; ω the angular frequency; c the speed of light in vacuum; and, $\epsilon(\mathbf{r})$ the periodically modulated dielectric function. The magnetic fields and the dielectric function can be expanded in terms of Fourier series as

$$\mathbf{H}(\mathbf{r}) = \sum_{\mathbf{G}}\sum_{\lambda=1}^{2} h_{\mathbf{G},\lambda}\hat{\mathbf{e}}_\lambda e^{i(\mathbf{k}+\mathbf{G})\cdot\mathbf{r}}, \tag{2}$$

$$\epsilon(\mathbf{r}) = \sum_{\mathbf{G}} \epsilon(\mathbf{G}) e^{i\mathbf{G}\cdot\mathbf{r}}, \tag{3}$$

where $\mathbf{k}$ is the Bloch wave vector in the first Brillouin zone (FBZ), and $\mathbf{G}$ is the 2D reciprocal lattice vector. The polarization unit vectors $\hat{\mathbf{e}}_\lambda$ with $\lambda = 1, 2$ are perpendicular to $(\mathbf{k}+\mathbf{G})$ and $h_{\mathbf{G},\lambda}$ is the Fourier expansion component of the magnetic fields. The Fourier coefficient $\varepsilon(\mathbf{G})$ is given by

$$\epsilon(\mathbf{G}) = \frac{1}{A_{\text{cell}}}\int_{\text{cell}} \epsilon(\mathbf{r}) e^{-i\mathbf{G}\cdot\mathbf{r}}\, d\mathbf{r}, \tag{4}$$

where the integration is performed over the unit cell. For structures with a unit cell including veins centered at $\mathbf{u}_i$, the corresponding dielectric constant is expressed as

$$\epsilon^{-1}(\mathbf{r}) = \epsilon_b^{-1} + (\epsilon_a^{-1} - \epsilon_b^{-1})\sum_{\mathbf{R}} P_{\text{sq}}(\mathbf{r}-\mathbf{R}) + (\epsilon_a^{-1} - \epsilon_b^{-1})\sum_i \sum_{\mathbf{R}} P_v^{(i)}(\mathbf{r}-\mathbf{u}_i-\mathbf{R}), \tag{5}$$

where P_{sq} and P_v describe the probability of the square rod and veins, respectively, and $\mathbf{R}$ denotes the translation vector of the Bravais lattice, and

$$P_{\text{sq}}(\mathbf{r}) = \begin{cases} 1 & \text{for } \mathbf{r} \in \mathbf{R}_{\text{sq}}, \\ 0 & \text{for } \mathbf{r} \notin \mathbf{R}_{\text{sq}}, \end{cases} \tag{6}$$

$$P_v^{(i)}(\mathbf{r}) = \begin{cases} 1 & \text{for } \mathbf{r}-\mathbf{u}_i \in \mathbf{R}_v^{(i)}, \\ 0 & \text{for } \mathbf{r}-\mathbf{u}_i \notin \mathbf{R}_v^{(i)}, \end{cases} \tag{7}$$

where $\mathbf{R}_{\text{sq}}$ and $\mathbf{R}_v^{(i)}$ are the regions in the xy-plane defined by the cross-section of the square rod and the ith vein, respectively. The Fourier transforms of $\epsilon^{-1}(\mathbf{r})$ are given by

$$\epsilon^{-1}(\mathbf{G}) = \epsilon_b^{-1}\delta_{\mathbf{G}0} + (\epsilon_a^{-1} - \epsilon_b^{-1})S_1(\mathbf{G}) + (\epsilon_a^{-1} - \epsilon_b^{-1})\sum_i S_2^{(i)}(\mathbf{G})\cdot e^{-i\mathbf{G}\cdot\mathbf{u}_i}. \tag{8}$$

The structural factors $S_1(\mathbf{G})$ and $S_2^{(i)}(\mathbf{G})$ are then given by

$$S_1(\mathbf{G}) = \left(\frac{l^2}{a^2}\right)\ \text{Sinc}\left(\frac{G_x l}{2}\right)\ \text{Sinc}\left(\frac{G_y l}{2}\right) \tag{9}$$

with $\text{Sinc}(x) = \sin x/x$, and

$$S_2^{(i)}(\mathbf{G}) = \left(\frac{l_x^{(i)} l_y^{(i)}}{a^2}\right)\ \text{Sinc}\left(\frac{G_x l_x^{(i)}}{2}\right)\ \text{Sinc}\left(\frac{G_y l_y^{(i)}}{2}\right), \tag{10}$$

where $l_x^{(i)}$ and $l_y^{(i)}$ are the side-lengths of the ith vein in the x- and y-axes respectively.

The band structures are then determined by solving the following equation

$$\sum_{\mathbf{G}'} A(\mathbf{k}+\mathbf{G}, \mathbf{k}+\mathbf{G}')H(\mathbf{G}') = \omega^2 H(\mathbf{G}) \tag{11}$$

with

$$A(\mathbf{K}, \mathbf{K}') = \begin{cases} |\mathbf{K}||\mathbf{K}'|\epsilon^{-1}(\mathbf{K}-\mathbf{K}') \\ \quad \text{for the } E\text{-polarization state}, \\ \mathbf{K}\cdot\mathbf{K}'\,\epsilon^{-1}(\mathbf{K}-\mathbf{K}') \\ \quad \text{for the } H\text{-polarization state}, \end{cases} \tag{12}$$

where $\mathbf{K} = \mathbf{k}+\mathbf{G}$, $\mathbf{K}' = \mathbf{k}+\mathbf{G}'$. $\epsilon^{-1}(\mathbf{K}-\mathbf{K}') = \epsilon^{-1}(\mathbf{G}-\mathbf{G}')$ can be computed by solving the following equation

$$\sum_{\mathbf{G}''} \epsilon^{-1}(\mathbf{G}-\mathbf{G}'')\epsilon(\mathbf{G}''-\mathbf{G}') = \delta_{\mathbf{G}\mathbf{G}'}. \tag{13}$$

3. Results and discussion

The following parameters were used in the calculations: $\epsilon_a = 11.4$ appropriate for gallium arsenide (GaAs) at

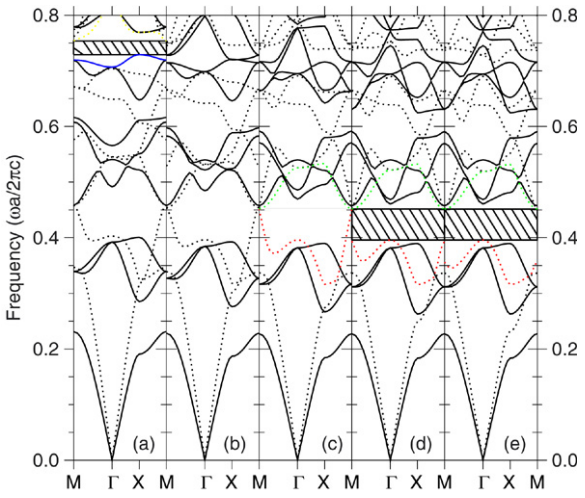

Fig. 2. Photonic band structures for five values of the vein length h — (a) $h = 0$ (i.e., the prototype structure without veins), (b) $h = 0.079a$, (c) $h = 0.155a$, (d) $h = 0.19a$ and (e) $h = 0.215a$. The relevant parameters are chosen as: $\epsilon_a = \epsilon = 11.4$, appropriate for GaAs material; $\epsilon_b = 1.0$ in air. The solid and dotted curves correspond to the E- and H-polarizations, respectively. The crosshatched area marks the complete gap region which lies between $E8$ (blue line) and $H7$ (yellow line) bands in (a), and $H2$ (red line) and $H3$ (green line) bands in (c)–(e). (For interpretation of the references to colour in this figure legend, the reader is referred to the web version of this article.)

wavelength $\lambda \approx 1.5$ μm and $\epsilon_b = 1.0$ in air. A Fourier expansion with 625 plane waves was used to calculate the PBGs for the $E(H)$-polarization and the convergence accuracy for the several lowest photonic bands was better than 1%. This study explored the influence of the growing veins on the photonic band gap formation. After extensive calculations, we have found that parameters with $l = 0.57a$ and $d = 0.08a$ provide the most dramatic improvement in the size of the complete PBGs. Fig. 2 depicts the calculated band structures when $l = 0.57a$ and $d = 0.08a$ for five different length of veins — (a) $h = 0$, (b) $h = 0.079a$, (c) $h = 0.155a$, (d) $h = 0.19a$ and (e) $h = 0.215a$, respectively. First, the PBG structures of the prototype square lattices with only square rods were calculated, as shown in Fig. 2(a). The solid (dotted) curves correspond to the $E(H)$-polarization. The diagram clearly shows four large PBGs for the E-polarization mode, i.e., the $E1$–2, $E3$–4, $E6$–7 and $E8$–9 gaps. For the H-polarization mode, only the $H6$–7 gap exists at higher index bands. The appearance of the $H6$–7 gap overlaps the $E8$–9 gap giving rise to a complete PBG with midgap frequency $\omega_g = 0.7415(2\pi c/a)$ and the gap size $\Delta\omega = 0.0246(2\pi c/a)$, as indicated by the crosshatched region. In contrast, when the square rods are linked with GaAs veins at each side of the square rods, the influences of the length h of the dielectric vein on the PBGs is investigated as shown in Fig. 2(b)–(e). It is clearly seen in Fig. 2(b) that the higher $E8$–9 gap disappears as the vein length h increases towards $0.079a$: thus the complete PBG closes. Furthermore, Fig. 2(c)–(e) shows that the $H2$–3 gap opens up for $h > 0.155a$ since the second H-polarization ($H2$) band moves towards lower frequencies at the **M** point of the Brillouin zone. When h increases up to $0.19a$, $H2$–3 gap is greatly enlarged, as shown in Fig. 2(d). We find an overlap between the $H2$–3 and $E3$–4 band gaps, with the former band gap completely covered by the latter band gap, leaving a complete PBG with the lower and upper band edges lying at the **Γ** (or **M**) and **M** symmetry points, respectively. This complete PBG reaches its maximum width with midgap frequency $\omega_g = 0.42385(2\pi c/a)$ and gap size $\Delta\omega = 0.0557(2\pi c/a)$. When h continues to increase and reaches $0.215a$ (the maximum value), the **M** point of the $H2$ band significantly shifts downwards below the **Γ** point (see Fig. 2(e)); however, the lower and upper band edges of this complete PBG remain almost unmodified, and lie at the **Γ** and **M** symmetry points, respectively. From Fig. 2(a)–(e) one sees that the gap widths of E-polarization at higher frequencies ($E8$–9 gap) and H-polarization at lower frequencies ($H2$–3 gap) strongly depend on the length of slender veins. Its existence reinforces the rule of thumb for PBGs that a PBG for E-polarization is favored in the case of a lattice of isolated high-ϵ regions, while a PBG for H-polarization is favored if the dielectric regions are connected [5]. Remarkably, the $E9$ band shifts downwards when the square rods are linked with a short length of veins at each side of the square rods (see Fig. 2(a) and (b)). If h increases further, the frequencies of $H2$ band at **M** symmetry point decreases quite rapidly (see Fig. 2(c)–(e)). These results can be interpreted by considering the effects of Mie scattering of the rod and the interaction of EM waves between neighboring rods to be significantly modified and enhanced when introducing the extra slender veins. If the length of veins increases, the Mie scattering of the rods would be modified to change the character of resonance frequency on the photonic bands. Notably, extending the length of veins substantially shrinks the complete PBG located at higher index bands, and generates the new complete PBG at lower index bands for an appropriate length of veins.

The complete PBG is an interesting issue for the extra veins formed on rods. First, the PBG map as a function of length of veins, h, is presented in Fig. 3(a). The parameters are as those quoted in Fig. 2 (i.e., $\epsilon_a = 11.4$, $l = 0.57a$, $d = 0.08a$). Only the first ten-bands are involved in this map for both E- and H-polarizations. The black region indicates the complete PBG. The gap map for E-polarization exhibits four large gaps. Significantly, the gaps tend to decrease in size at higher frequencies. For the H-polarization modes, two remarkable gaps occur: the higher one is in the range $h = [0, 0.215]a$, while the lower one appears for $h = [0.155, 0.215]a$. It is clear that these two H-polarization gaps overlap with other E-polarization gaps; thus, two complete PBGs are obtained in the range $h = [0, 0.079]a$ for the higher one and $h = [0.155, 0.215]a$ for the lower one. Second, the evolution of edge states of the lower complete PBG as a function of the vein length h is plotted in Fig. 3(b). According to the calculation of the photonic band structures, the edge states of the lower complete PBG lie at high symmetry points of the Brillouin zone as $H^{(2,\mathrm{M})}$, $H^{(3,\mathrm{M})}$, $H^{(4,\mathrm{M})}$ and $H^{(2,\Gamma)}$. Herein, $H^{(n,\mathrm{M})}$ and $H^{(n,\Gamma)}$ denote the nth bands for the H-polarization mode at **M** and **Γ** points. The $H^{(2,\mathrm{M})}$ and $H^{(3,\mathrm{M})}$ bands are degenerate in the region given by $h = [0, 0.215]a$ and their frequencies remain almost unmodified at around $0.452(2\pi c/a)$. Moreover, the other $H^{(2,\Gamma)}$ band's frequency also remains

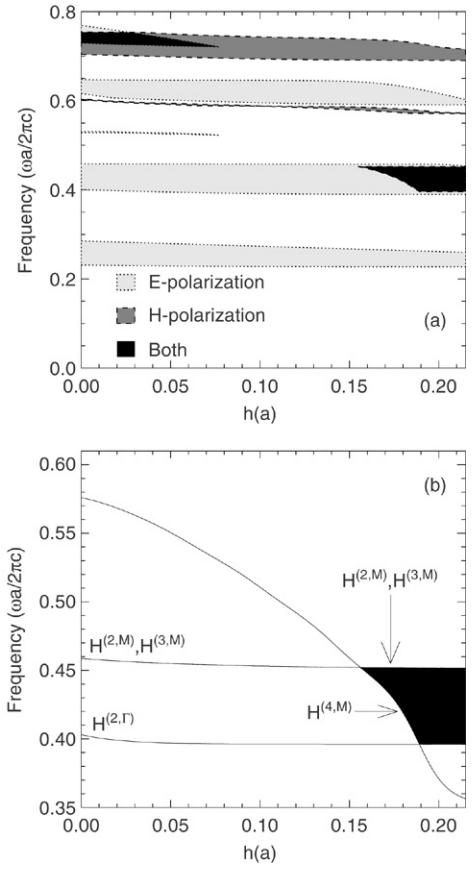

Fig. 3. (a) Gap map of the proposed PC, as the vein length h varies for both E- and H-polarizations. The parameters are as those quoted in Fig. 2 (i.e., $\epsilon_a = 11.4$, $l = 0.57a$, $d = 0.08a$). The black area denotes the complete band gaps. (b) The evolution of edge states of the lower complete PBG as a function of vein length, h. $H^{(n,\mathrm{M})}$ and $H^{(n,\Gamma)}$ denote the nth bands for the H-polarization mode at **M** and **Γ** points of the Brillouin zone.

almost unchanged at around $0.396(2\pi c/a)$. The frequencies of $H^{(4,\mathrm{M})}$ decrease significantly for increasing h. As the $H^{(4,\mathrm{M})}$ band is below $H^{(2,\mathrm{M})}$ and $H^{(3,\mathrm{M})}$ bands for $h > 0.155a$, the lower complete PBG is opened, and its width increases quite sharply. In the region $h > 0.155a$, the complete PBG is bounded on the lower side by the $H^{(4,\mathrm{M})}$ boundary (i.e., **M** point of the $H2$ band shown in Fig. 2(c) and (d)), and on its upper side by the $H^{(2,\mathrm{M})}$ or $H^{(3,\mathrm{M})}$ boundary (i.e., **M** point of $H3$ and $H4$ bands shown in Fig. 2(c)–(e)). Furthermore, the vein length increases up to about $h = 0.19a$, and the $H^{(4,\mathrm{M})}$ band is again lower than the $H^{(2,\Gamma)}$ band. The complete PBG is thus bounded on the lower side by the $H^{(2,\Gamma)}$ boundary, and on its upper side by the $H^{(2,\mathrm{M})}$ ($H^{(3,\mathrm{M})}$) boundary in the region $h = [0.19, 0.215]a$. Notably, this complete PBG tends to increase in size dramatically in the region $h = [0.155, 0.19]a$, and reaches its maximum value at $h = 0.19a$. Then, the frequencies of the lower and upper edges of this complete PBG remain almost unchanged in the region $h = [0.19, 0.215]a$. Finally, it is worth pointing out the d (the width of the vein) dependence of the band structure. When the veins are fully connected at the lattice unit cell boundary, the extreme situation that the width of vein is large enough to have veins (dielectric constant the same as that of square rods) contacted or covering each other to form the closed-packed structure. In such a case, there are no gaps for any polarization. In the thin vein, we present in this paper, the complete PBG really existed. Hence, the width of the vein is shown to affect the band structures and band gaps.

4. Conclusion

This study proposes two-dimensional PCs of a square lattice with dielectric square rods growing veins on the middle of each side of dielectric square rods in air. Such PCs can be fabricated by separately building two 2D PCs, with one PC consisting of dielectric square rods located at the center of a square lattice, and the other PC consisting of four dielectric veins located at the middle of each side of the dielectric square rod. The two PCs are then combined into a final interpenetrating structure. The photonic band gaps are affected by the characteristics of the veins by considering the effects of Mie scattering and interference of EM waves. Properly adjusting the length of the dielectric veins enables the *complete* PBG generated from the composite structure to be closed and opened. Additionally, the complete PBG reaches its maximum value where the veins are nearly connected with each other. Our results may provide a new direction for designing PBG of two-dimensional photonic crystals.

Acknowledgements

The authors would like to thank the National Science Council of the Republic of China, Taiwan (Contract No. NSC94-2112-M-009-001) and the Electrophysics Department, National Chiao Tung University, Taiwan, for their support. We acknowledge Ben-Yuan Gu for discussions.

References

[1] E. Yablonovitch, Phys. Rev. Lett. 58 (1987) 2059.
[2] S. John, Phys. Rev. Lett. 58 (1987) 2486.
[3] S. John, Nature 390 (1997) 661.
[4] C.M. Soukoulis (Ed.), Photonic Band Gaps and Localization, Plenum, New York, 1993.
[5] J.D. Joannopoulos, R.D. Meade, J.N. Winn, Photonic Crystals—Molding the Flow of Light, Princeton University Press, 1995.
[6] E. Yablonovitch, Sci. Am. 285 (6) (2001) 34.
[7] K. Sakoda, Optical Properties of Photonic Crystals, Springer-Verlag, 2001.
[8] C.T. Chan, S. Datta, K.M. Ho, C.M. Soukoulis, Phys. Rev. B 50 (1994) 1988.
[9] S. Fan, P.R. Vileneuve, R.D. Meade, J.D. Joannopoulos, Appl. Phys. Lett. 65 (1994) 1466.
[10] C.M. Anderson, K.P. Giapis, Phys. Rev. Lett. 77 (1996) 2949.
[11] X.H. Wang, B.Y. Gu, Z.Y. Li, G.Z. Yang, Phys. Rev. B 60 (1999) 11417.
[12] Z.Y. Li, B.Y. Gu, G.Z. Yang, Phys. Rev. Lett. 81 (1998) 2574; Eur. Phys. J. B 11 (1999) 65.
[13] D.F. Sievenpiper, E. Yablonovitch, Phys. Rev. Lett. 80 (1998) 2829.
[14] W.Y. Zhang, X.Y. Lei, Z.L. Wang, D.G. Zheng, W.Y. Tam, C.T. Chan, P. Sheng, Phys. Rev. Lett. 84 (2000) 2853.
[15] M.M. Sigalas, C.M. Soukoulis, R. Biswas, K.M. Ho, Phys. Rev. B 56 (1997) 959.
[16] C.S. Kee, J.E. Kim, H.Y. Park, Phys. Rev. E 57 (1998) 2327.
[17] B. Gates, Y. Xia, Adv. Mater. 13 (2001) 1605.

[18] S.I. Bozhevolnyi, D.J. Erland, K. Leosson, P.M.W. Skovgaard, J.M. Hvam, Phys. Rev. Lett. 86 (2001) 3008.
[19] S. David, A. Chelnokov, J.-M. Lourtioz, IEEE J. Quant. Elect. 37 (2001) 1427.
[20] T. Pan, Z.-Y. Li, Solid State Commun. 128 (2003) 187.
[21] M. Qiu, S. He, J. Opt. Soc. Am. B 17 (2000) 1027.
[22] R.L. Chern, C.C. Chang, C.C. Chang, R.R. Hwang, Phys. Rev. E 68 (2003) 026704.
[23] M. Maldovan, E.L. Thomas, J. Opt. Soc. Am. B 22 (2005) 466.
[24] K.M. Ho, C.T. Chan, C.M. Soukoulis, Phys. Rev. Lett. 65 (1990) 3152.
[25] Z. Zhang, S. Satpathy, Phys. Rev. Lett. 65 (1990) 2650.
[26] K.M. Leung, Y.F. Liu, Phys. Rev. Lett. 65 (1990) 2646.
[27] C.-S. Kee, J.-E. Kim, H.Y. Park, Phys. Rev. E 56 (1997) R6291.
[28] H.C. Van de Hulst, Light Scattering by Small Particles, Wiley, New York, 1957.